Sequential Thermal Dissolution of Naomaohu Brown Coal

[1]Bingbing Song and [2]Yangyang Zhang,
[1,2]College of Chemistry and Chemical Engineering, Henan Polytechnic University, Jiaozuo, Henan, China

Abstract—Sequential thermal dissolution of Naomaohu (NL) brown coal in cyclohexane, methanol, ethanol and isopropanol was conducted at 300 $^{\circ}$C for 2 h in turn. All soluble parts (SP_1-SP_4) were analyzed by gas chromatography/mass spectrometer. NL was analyzed by thermogravimetric analysis (TG). Thermal dissolution residue (ER_4) was analyzed by Fourier transform infrared spectroscopy (FTIR), X-ray photoelectron spectroscopy (XPS). As a result, NL underwent a strong bond breaking process between 400-500 $^{\circ}$C, mainly the breakage of covalent bonds such as Calk-C, Calk-H, Cak-O and Car-N. The existence of COO species in ER_4 indicated that methanol, ethanol and isopropanol might be esterified or ester-exchanged with carboxylic acid, while the reduced C-O species illustrated that the nucleophilic oxygen atom in methanol, ethanol and isopropanol attacked the carbon atom on the carbonyl group in NL. By GC/MS, compounds detected in SP_1 are mainly alkanes, alkenes, and aromatics, while phenols predominant in SP_2, alcohols and esters are dominant in SP_3, and alkanes are mainly found in SP_4. It is noteworthy that NCOCs relatively high in SP_2, and SCOCs were detected only in SP_2 and SP_3.

Keywords—Cyclohexane; Methanol; Ethanol; Isopropanol; Brown Coal

I. INTRODUCTION

Lignite are an important fossil energy resource and are widely distributed around the world[1–4], but they are considered to be subpar fuel sources due to their high ash yield, abundant water content, low calorific value, high volatile matter content, and high sulfur content[5,6] Not only does it have low combustion efficiency, but it also has negative impacts on the environment and people's health[7]. Therefore, it is necessary to find an efficient method to make up for these drawbacks.

Over the past few decades, there have been numerous studies on the pyrolysis[8], oxidation[9,10] and liquefaction[10,11] of lignite. However, the sequential thermal dissolution of lignite under mild conditions is also worth paying attention to. By sequential thermal dissolution, valuable chemical substances can be enriched and separated from lignite[12,13]. Besides, low-boiling solvents (such as Cyclohexane[14,15], methanol[15], ethanol[16] and isopropanol) are widely used in lignite thermal dissolution due to their easy recyclability. Low boiling point solvents such as cyclohexane do not react with the organic matter in coal, and can obtain the composition structure information coal more objectively[15]. Low carbon alkyl alcohols such as methanol, ethanol and isopropanol can break the weak covalent bonds (such as -C-O-) due to their own nucleophilicity, which makes more organic matter depolymerize. This process not only lays the foundation for an in-depth understanding of the molecular composition of coal, but also provides a guarantee for the rational use of coal. Therefore, in this paper, inert solvent cyclohexane low carbon alkyl alcohols (methanol, ethanol and isopropanol) are used to gradually increase the temperature for mild thermal dissolution of lignite, in order to the organic matter in coal layer by layer, and obtain complete molecular composition information and the dissociation and depolymerization process of organic matter.

A thorough understanding of the chemical structure of coal is of great significance for its efficient utilization, especially in obtaining high-value chemicals from coal However, the structure of coal is too complex to be described in detail. It is common to use characterization tools such as elemental analysis, Fourier transform infrared spectroscopy (FTIR)[5], X-ray photoelectron spectroscopy (XPS)[17], gas chromatography-mass spectrometry (GC/MS)[15] to understand the structural information of coal. The use of these tools for analysis has greatly facilitated the understanding of the composition of elements, functional groups, forms of oxygen, nitrogen, and sulfur in coal, as well as the analysis of the chemical composition of the soluble fraction. In addition, thermogravimetric analysis (TGA)[18] is widely used in the study of coal pyrolysis behavior.

In this study, NL was conducted to sequential thermal dissolution, and the soluble and insoluble components were obtained. The chemical structure of NL and the thermal dissolution residues were characterized using direct techniques such as XPS, TGA, and FTIR. Additionally, the chemical composition of the soluble fraction was analyzed by identifying the filtrate using GC/MS. The aim of this study was to obtain information on the overall structure of the experimental coal samples. This study provides a reliable theoretical basis for the directed conversion of organic matter into chemicals, especially in medium to low-rank coals.

II. EXPERIMENTAL

A. Materials

NL was collected from Nao Maohu, Inner Mongolia, China, and pulverized to pass through a 200-mesh sieve (particle size of <74 μ m) followed by desiccation in a vacuum at 80 $^{\circ}$C for 24 h before use. The industrial analysis and elemental analysis of the coal samples used in the experiment are shown in Table 1. All the solvents used in the experiment were commercially purchased analytical reagents and purified by distillation prior to use.

TABLE I.
PROXIMATE AND ULTIMATE ANALYSES OF NL (WT%)

Proximate analysis			Ultimate analysis				$S_{t,d}$
M_{ad}	A_d	VM_{daf}	C	H	N	O_{diff}	
4.54	7.44	48.97	62.41	4.84	0.98	31.01	0.76

B. Sequential thermal dissolution procedure

NL was exhaustively extracted with isometric carbon disulfide/acetone mixed solvent to obtain extract solution and residue (ER). As shown in Fig. 1, about 6 g ER and 20 mL solvent (cyclohexane） were placed into a 100 mL magnetically stirred autoclave. After replacing air with N_2, the autoclave was heated to 300 $^{\circ}$C at 5 $^{\circ}$C min^{-1} and maintained at

300 °C for 2 h. Then, the autoclave was cooled to room temperature, and the reaction mixture was taken out from the autoclave and separated into filtrate (SP₁) and filter cake (ER₁) by filtration. The filter cake was exhaustively extracted with acetone/carbon disulfide solvent. Then, methanol, ethanol and isopropanol were used as solvents, and the above operations were repeated to sequential thermal dissolution the insoluble matter after cyclohexane thermal dissolution.
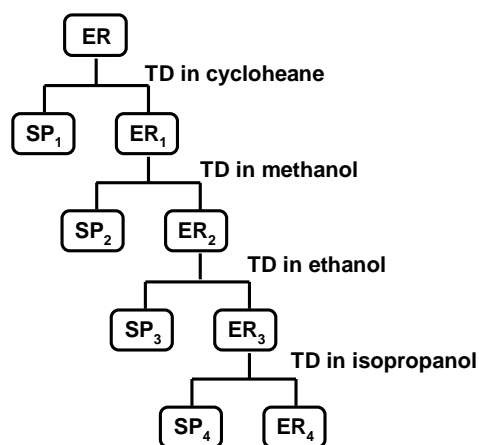
Fig. 1. Procedure for ER sequential thermal dissolution

C. Characterization

The surface elemental composition of coal samples was detected by a Thermo Fisher ESCALAB 250Xi XPS, which analyze the type, quantity, and chemical speciation of elements on the surface of a sample The ray source is Al K α (hv = 1486.6 eV), the pressure in the analytical chamber is 5×10^{-9} Pa, and the grazing angle (the angle between the direction of electrons entering the analyzer and the sample) is measured at 30°. The energy correction of O, N and S is based on the standard C 1s electron binding energy of 284.8 eV. Peak fitting and semi-quantitative analysis of the narrow spectra of different elements were performed using XRPES Peakfit software.

The NETZSCH STA 449 F5 synchronous thermal analyzer was used for thermogravimetric analysis of coal samples. The sample was about 10 mg, and the heating rate of the instrument was 10 °C/min, and the heating program was two consecutive stages of gradient heating, the first stage was heated to 110 °C for 10 min, and the second stage was continued to be heated to 900 °C for 20 min. Origin 9.0 software was used to plot the obtained TG curves.

FTIRS was used to analyze the composition of functional groups in the coal samples, the coal samples were mixed with KBr, and then pressed into thin slices with good light transmission with a tablet press and put into the instrument for detection. The instrument has a scanning range of 700‑4000 cm⁻¹, 32 scans, and a spectral resolution of 4 cm⁻¹.

Agilent 7890/5975 GC/MS was used to qualitatively and quantitatively analyze the chemical composition of small molecules in SPs. GC/MS used high-purity He (99.999%) as the mobile phase carrier gas with a flow rate of 1.0 mL min-1, GC advance port temperature of 250 °C, HP-5MS column with column length of 60 m, inner diameter of 250 μ m, and film thickness of 0.25 μ m, electron bombardment ionization source (EI) with ionization voltage of 70 eV and temperature of 230 °C, quadrupole mass analyzer temperature of 150 °C, and ion mass scan range of 33-550 u. The compound's molecular structure was determined by comparing its mass spectra with those in the NIST11a spectral library. For compounds with challenging structures, identification can also rely on retention time from the total ion chromatogram and comparisons of base,

fragment, molecular, and isotopic peaks in the mass spectrum with reference data.

III. RESULTS AND DISCUSSION

A. Analysis of NL with TGA

As can be seen from the TGA curve of NL in Fig. 2, the weight loss of NL can mainly divide into three stages. The first stage is from 100 to 420 °C, with a relatively gentle weight loss and a weight loss of only about 8%. The second stage is from 420 to 700 °C, with a gradually rapid weight loss, reaching 32%. The third stage is from 700 to 900 °C, with the weight loss rate of NL beginning to decrease and then becoming gentle, reaching 5%. The total mass loss of NL is 45%. The DTG curve of the sample was fitted by PeakFit 4.0 software and a total of 7 peaks were fitted. By consulting the literature[18], the 7 peaks were simply summarized as shown in Table 2. As be seen from Fig. 2, Peak 1 is between 100 and 180 °C and a very low relative content, indicating NL contains a small amount of bound water, which is consistent with the moisture results of the air-dried basis in the industrial analysis. The second peak between 180-300 °C, with bond energies between 150-230 kJ/mol represents the decomposition of carboxyl groups in the coal sample, indicating that the coal sample contains a large amount of >C=O and COO groups. Peak 3 at 300-400 °C can be attributed to the breakage of Cal-X (X=O, N, S) in brown coal, which is theage of weak covalent bonds and weak bridge bonds between aliphatic and heteroatoms. Peak 4 is between 400 and 500 °C, and it can be easily seen and its relative content is the highest, which may be due to the breakage of weak covalent bonds of Cal-Cal, Cal-H, Cal-O and Cal-N bonds in brown coal. With the gradual increase in temperature, Peak 5 is attributed to the breakage of Car and Cal, O and S, which are the breakage of aromatic bridge bonds. Peaks 6 and 7 belong to the decomposition of minerals and the condensation of aromatic rings. In this process, the decomposition of carbonates in brown coal will produce CO_2, and the condensation of aromatic rings may lead to the release of H_2
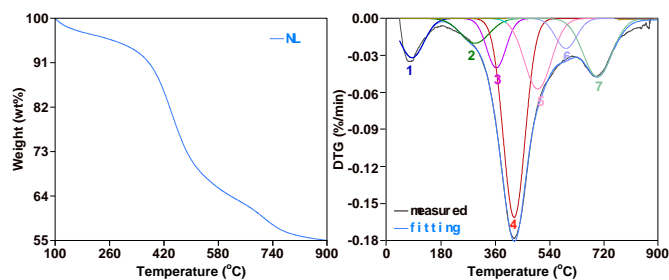
Fig. 2 TG curve and DTG fitting curves of NL

TABLE II.
ASSIGNMENT OF PEAKS FORMS DTG ANALYSIS OF NL

Peak	Peak temperature (°C)	Bond range (kJ/mol)	Origin
1-2	< 300	< 150	Release of bonded water and decomposition of carboxylic acid
3	300-400	150-230	Breakage of bonds between Cal and O, S and N, and S-S
4	400-500	210-320	Breakage of bonds between Cal and Cal, H, O, and Car-N
5	500-600	300-430	Breakage of bonds between Car and Cal, O and S
6	~700	-	Decomposition of carbonates in coals to generate CO_2
7	700-800	> 400	Condensation of aromatic rings to release H_2

B. Ultimate Analysis

As shown in Table 3, the C content of NL is 62.41%, and the oxygen content is as high as 31.01%. The high oxygen

content is the main reason for the low calorific value, which also hinders the industrial application of low-rank coal[13]. Compared with NL, the O content of ER has significantly decreased, while the change in C content is relatively small, indicating that extraction has a significant effect on the dissolution of oxygen compounds in NL. However, the S relative content of NL is low, it significantly increases after extraction, which may be due to the difficulty of extracting S compounds, and the residue of carbon disulfide during extraction. After extraction, ER undergoes further sequential thermal dissolution. The C content decreases slightly after sequential thermal dissolution, while the O content decreases significantly, indicating that sequential thermal dissolution has a good effect on the dissolution of oxygen compounds or oxygen bridges in coal. The S content in the thermal dissolution residue also increases significantly, indicating that under the conditions of heating and pressure, S-containing compounds are also difficult to dissolve, sequential and thermal dissolution, it is further enriched in the thermal dissolution residue.

TABLE III.
ULTIMATE ANALYSIS (DAF) OF NL、ER AND ER_4

Samples	C	H	N	O_{diff}	$S_{t, d}$	H/C
NL	62.41	4.84	0.98	31.01	0.76	0.93
ER	64.84	4.44	0.47	23.83	6.43	0.83
ER_4	61.99	4.23	0.52	15.17	18.09	0.82

C. Analysis of NL and ER_4 with FTIR

FTIR can directly analyze the organic structures in complex mixtures to obtain information about the overall structure of the sample. As depicted in Fig. 3, the spectrum of NL contains multiple distinct absorption peaks, while the spectrum of ER_4 shows a decrease or disappearance in the intensity of some absorption peaks. This indicates that certain components in the coal sample were removed or decomposed after sequential thermal dissolution. Strong absorbances from bound -OH (3444 cm^{-1}), aromatic rings 1629 cm^{-1}) and aliphatic moieties (2928 and 2871 cm^{-1}) appear in ZL and ER_4 and there is no obvious difference in such absorbances between ZL and ER_4. This indicates suggests that ZL and ER_4 have similar aromaticity indexes. The absorption peak near 1105 cm^{-1} is attributed to the -COOH group. Compared to NL, the peak of ER_4 is sharper, which may be due to a reduction in the content of COOH. The significant difference in peak intensity around 612 cm^{-1} reflects the varying degree of substitution of aromatic compounds.
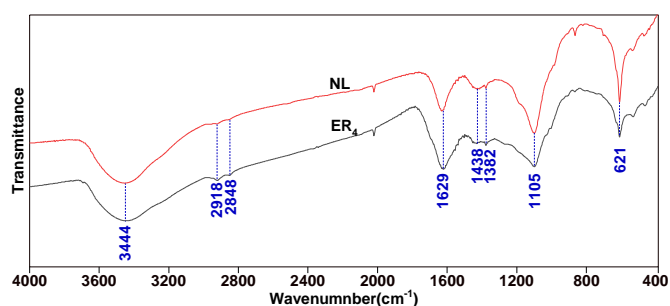
Fig. 3. FTIR spectrum of NL and ER_4

D. Analysis of ER and ER_4 with XPS

According to the elemental analysis results, the changes in various elements are significant after the extraction process and sequential thermal dissolution. Therefore, understanding the changes in element forms during sequential thermal dissolution is crucial for understanding the impact of the dissolution process on coal structure. XPS is used to characterize the surface element composition of coal and its residues. As shown in Fig. 4 and Table 4, the forms and molar contents of C, O,

and N elements on the solid surfaces of NL and ER_4 are significantly different.

The XPS C 1s spectra of NL and ER_4 were fitted with five peaks in the form of carbon atoms: C-C, C-H, C-O, C=O and COO. Compared with NL, the ratio of C-O content in ER_4 is relatively low, which may be due to the destruction of C-O during the thermal dissolution process with alcohol solvents

The XPS O 1s spectra of NL and ER_4 both fit peaks corresponding to four oxygen atomic forms: C=O, -OH, C-O, and COOH. It can be observed that the molar contents of carbonyl and hydroxyl groups increase significantly, while ether bonds and carboxyl groups decrease noticeably. This indicates that ether bond oxygen and carboxyl oxygen are transferred to soluble components after sequential thermal dissolution, and ether bond oxygen may be may be the attack of oxygen atoms in alcohols on the -CH$_2$-, resulting in the destruction of C-O species[13] and carboxyl oxygen may be dissolved by esterification reaction with alcohol solvents, as shown in Scheme 1. This is consistent with the corresponding evidence in FTIR.

The N 1s in ER and ER_4 includes pyridine, amino nitrogen, Pyrrolic nitrogen, Quaternary nitrogen and Chemisorbed nitrogen oxides, corresponding to the peak positions of 394.9, 399.3, 400.2, 401.2 and 402.8 eV.

Scheme 1: Possible pathways of the esterification or transesterification reactions of ER in the sequential thermal dissolution process (R represent H, an alkyl, or and aryl group, R1 represents methyl or ethyl).
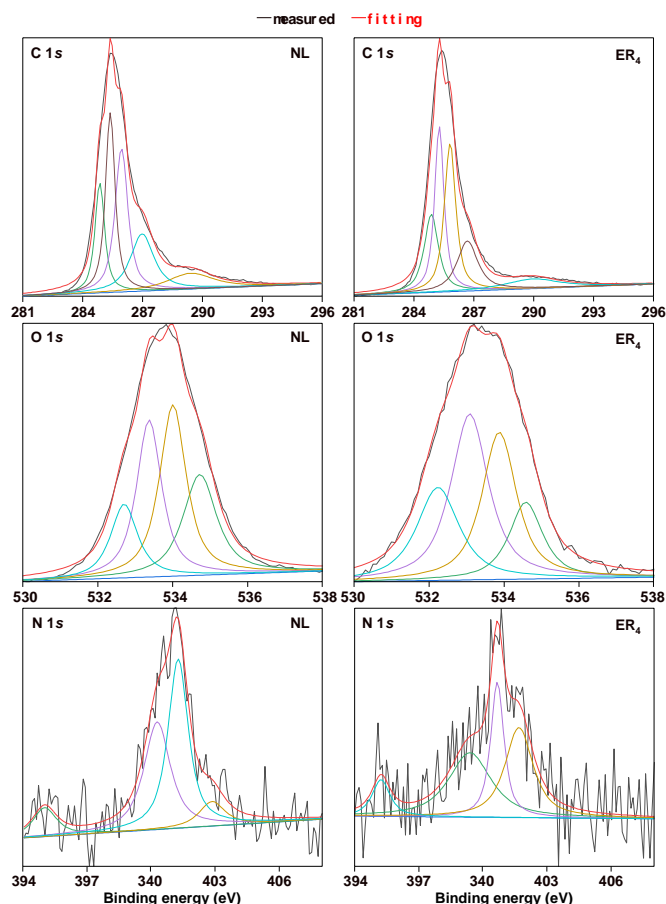
Fig. 4 XRPES C 1s, O 1s, and N 1s spectra and their fitting curves of NL and ER_4

TABLE IV.
DISTRIBUTIONS OF O, N, AND S FORMS ON THE SURFACE OF NL AND ER₄ DETERMINED BY XPS

Elemental peak	Binding energy(eV)	Functionality	Molar content (%) NL	Molar content (%) ER₄
C 1s	284.8	C-C	15.82	18.86
	285.2	C-H	25.81	28.56
	285.8	C-O	27.50	26.57
	286.9	C=O	20.01	17.34
	289.3	COO	10.85	8.67
O 1s	532.0	C=O	14.29	22.00
	532.7	-OH	28.26	35.04
	533.4	C-O	33.05	28.46
	534.2	COOH	24.40	14.49
N 1s	394.9	Pyridinic nitrogen	9.82	10.06
	399.3	Amino nitrogen	8.88	24.69
	400.2	Pyrrolic nitrogen	32.18	25.36
	401.2	Quaternary nitrogen	34.92	20.29
	402.8	Chemisorbed nitrogen oxides	14.21	19.60

E. Analysis of filtrates with GC/MS

According to GC/MS analysis, 140, 137, 90, and 54 organic compounds were detected in SP_1-SP_4, respectively. They can be classified into alkanes, alkenes, aromatics, alcohols, phenols, ketones, esters, nitrogen-containing organic compounds (NCOCs), sulfur-containing organic compounds (SCOCs), and other compounds (OCOCs). As illustrated in Fig. 5, compounds detected in SP_1 are mainly alkanes, alkenes, and aromatics, while phenols predominant in SP_2, alcohols and esters are dominant in SP_3, and alkanes are mainly found in SP_4. It is noteworthy that NCOCs relatively high in SP_2, and SCOCs were detected only in SP_2 and SP_3. Detailed analysis of the types of substances is summarized in Table 5-18, and the ion chromatogram is shown in the attached Fig 6-9.
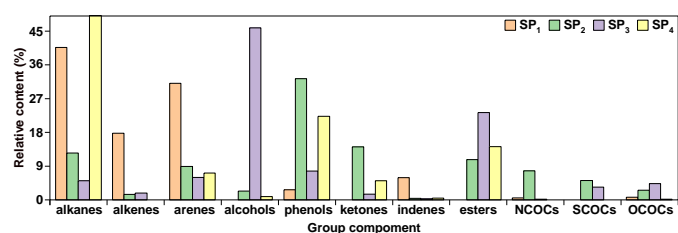
Fig. 5 Distribution of group components released from sequential thermal dissolution of NL

As shown in Tables 5-7, the alkanes in SPs can be classified into normal alkanes, branched alkanes, and cycloalkanes, with a carbon number distribution ranging from C_7-C_{26}. As the thermal dissolution progresses, the types of dissociated alkanes decrease, with most alkanes being liberated from intermolecular forces during the cyclohexane thermal dissolution process. As shown in Table 8, alkenes are primarily detected in SP_1-SP_3, SP_1 is the most abundant, contains dienes and alkenes, and the content is relatively rich in long-chain alkenes, while only 4 types (1,5-dimethylcyclopent-1-ene, 1,2,3-trimethylcyclopent-1-ene, 1,2,4,4-tetramethylcyclopent-1-ene and 6,6-dimethylhepta-2,4-diene) detected in SP_2, and 2 types((E)-1-ethoxybut-1-ene and 1-ethoxyhexa-2,4-diene) detected in SP_3. It can be found that SP_2 and SP_3 detect the alkenes and diolefins with short chains, and it is speculated that the π bonds of the long-chain alkenes are easily broken by thermal action and can be dissolved in large quantities in SP_1, while the short-chain alkenes and dienes are easily bound to the capsule junction in

the coal due to their own structure. It is difficult to destroy their interaction with the coal structure, and thermal and polar solvents methanol and ethanol are required to interact with them, on the other hand, short-chain olefins are mainly dissolved at higher temperatures. It may also be generated by the breaking reaction of long chains.

TABLE V.
NAMES AND CONTENT OF NORMAL ALKANES DETECTED WITH GC/MS

Peak number	Names	Relative content (%) SP₁	SP₂	SP₃	SP₄
2	heptane	0.25			
10	octane	0.47			
20	nonane	0.59			
29	decane	0.53			
43	undecane	0.44	0.10		
57	dodecane	1.09			
71	tridecane	0.65		0.63	
78	tetradecane	2.27	0.46	0.63	3.06
83	hexadecane	5.49	1.59	0.80	6.53
85	pentadecane	4.77	1.47	1.06	8.29
92	heptadecane	2.70	0.85	0.39	3.74
98	octadecane	2.49	0.63		1.33
100	nonadecane	1.67	0.68		
103	eicosane	1.66	0.42		
105	heneicosane	2.04	0.67		
106	docosane	1.71	0.57		
108	tricosane	2.00	0.45		
110	tetracosane	1.68	0.40		
112	hexacosane	1.04			
113	pentacosane	0.74			

TABLE VI.
NAMES AND CONTENT OF BRANCHED ALKANES DETECTED WITH GC/MS

Peak number	Names	Relative content (%) SP₁	SP₂	SP₃	SP₄
15	2,3-dimethylheptane	0.29			
22	3-ethyl-2-methylheptane	0.66			
59	2,6-dimethylundecane	0.41			
90	2,6,10-trimethylpentadecane	0.64			
93	2,6,10,14-tetramethylpentadecane	1.12		0.46	
197	2,6,10-trimethylhexadecane		0.87		3.39
259	2,6,10,14-tetramethylhexadecane			0.21	1.58
277	2,3,7-trimethyldecane				2.78

TABLE VII.
NAMES AND CONTENT OF CYCLOALKANES DETECTED WITH GC/MS

Peak number	Names	Relative content (%) SP₁	SP₂	SP₃	SP₄
4	methylcyclohexane	0.39			
5	1,2,3-triethylidenecyclopropane	0.23			
6	1-methyl-1-(prop-1-en-2-yl)cyclopropane	0.85			
13	vinylcyclohexane	0.24			
14	ethylcyclohexane	0.25			
96	1-butyl-2-propylcyclopentane	1.01			

101	cyclotetradecane	0.15		
111	cyclohexadecane	0.35		
114	cyclohexane		3.36		17.51
215	Isopropenylcyclopropane			0.91	
266	(1R,2R)-1,2-dimethyl-3-methylenecyclopentane				1.23

TABLE VIII.
NAMES AND CONTENT OF CYCLOALKANES DETECTED WITH GC/MS

Peak number	Names	Relative content (%)			
		SP$_1$	SP$_2$	SP$_3$	SP$_4$
1	cyclohexene	9.57			
3	1,5-dimethylcyclopent-1-ene	1.01	0.63		
8	1-methylcyclohex-1-ene	1.30			
9	oct-2-ene	0.26			
11	1,2,3-trimethylcyclopent-1-ene	0.51	0.46		
12	1-ethyl-2-methylcyclopent-1-ene	0.34			
16	2,6-dimethylhepta-2,4-diene	0.47			
19	non-1-ene	0.42			
27	dec-1-ene	0.17			
94	7-methyltridec-6-ene	0.36			
97	octadec-1-ene	1.51			
99	nonadec-9-ene	0.34			
104	henicos-10-ene	0.84			
107	tricos-1-ene	0.52			
109	(Z)-tricos-9-ene	0.31			
122	1,2,4,4-tetramethylcyclopent-1-ene		0.27		
123	6,6-dimethylhepta-2,4-diene		0.14		
211	(E)-1-ethoxybut-1-ene			1.60	
227	1-ethoxyhexa-2,4-diene			0.23	

As shown in Tables 9-11, a variety of different alkyl group substitutions and different aromatic ring numbers make the diversity of aromatic ring compounds. It can be observed that the number of aromatic rings ranges from 1 to 3, and 3-ring aromatics detected only in SP$_1$ and SP$_2$. Aromatics in SPs are mainly detected in SP$_1$, while their relative content in SP$_2$-SP$_4$ is not high. Methanol, ethanol, and isopropanol are polar solvents and do not form conjugated structures with double bonds or aromatic rings, which makes it difficult to separate aromatics from them structurally and also may be due to the fact that the small molecular weight aromatic hydrocarbons have been largely dissolved in cyclohexane. Based on the solubility rules of aromatic hydrocarbons, it is speculated that there two possible sources of aromatic hydrocarbons: one is from the aromatic hydrocarbons existing in the structure of NL itself; on the other hand, since the aromatic hydrocarbons in the hot solvents are mostly methyl-substituted aromatic hydrocarbons, they be due to the breakage of the C_α-C_β bond of the straight-chain alkylbenzene at high temperature.

TABLE IX.
NAMES AND CONTENT OF MONOCYCLIC AROMATIC HYDROCARBONS DETECTED WITH GC/MS

Peak number	Names	Relative content (%)			
		SP$_1$	SP$_2$	SP$_3$	SP$_4$
7	toluene	5.78	0.43	1.30	1.37
17	ethylbenzene	1.47	0.42		0.64
18	m-xylene	3.00	0.54		1.87
21	cumene	0.34			0.29
23	propylbenzene	0.32			
24	1-ethyl-3-methylbenzene	1.54			
25	mesitylene	0.12	0.26	0.47	1.69
28	1,2,3-trimethylbenzene	2.27			
30	o-cymene	0.52			
31	cyclopropylbenzene	0.68			
32	indene	0.14			
34	butylbenzene	0.28			
35	1-ethyl-2,3-dimethylbenzene	0.093	0.18		
36	1-methyl-2-propylbenzene	0.16			
38	2-ethyl-1,4-dimethylbenzene	0.36			
39	but-3-en-2-ylbenzene	0.06			
40	4-methyl-2,3-dihydro-1H-indene	1.07			
41	(E)-but-2-en-2-ylbenzene	0.58			
42	2-ethyl-1,3-dimethylbenzene	0.23			
45	2,4-diethyl-1-methylbenzene	0.19			
46	1-ethyl-2,4-dimethylbenzene	0.14			
48	4-isopropyl-1,2-dimethylbenzene	0.22			
50	1,2,4,5-tetramethylbenzene	0.30			
51	1-methyl-1H-indene	0.13			
52	pentylbenzene	0.13			
56	1,6-dimethyl-2,3-dihydro-1H-indene	0.40	0.40		
60	(E)-pent-1-en-1-ylbenzene	0.10			
63	1,2,3,4,5-pentamethylbenzene	0.11			
65	cyclopent-1-en-1-ylbenzene	0.13			
67	4,7-dimethyl-2,3-dihydro-1H-indene	0.50			0.49
68	2,3-dimethyl-1H-indene	0.30			
75	heptylbenzene	0.31			
76	hexa-2,4-dien-2-ylbenzene	0.28			
84	octylbenzene	0.31			
86	1,1,4,5,6-pentamethyl-2,3-dihydro-1H-indene	3.12			
125	p-xylene		0.28	2.35	1.14
130	1-ethyl-2-methylbenzene		0.20		
141	1,3-diethylbenzene		0.05		
145	1-ethyl-3-vinylbenzene		0.33	0.23	
154	(2-methylbut-1-en-1-yl)benzene		0.22		
164	1-ethyl-4-isopropylbenzene		0.95		
168	1-(but-2-en-1-yl)-2,3-dimethylbenzene		0.22		
186	1,4,5-trimethylnaphthalene		0.46		
190	1-(tert-butyl)-3-isopropyl-5-methylbenzene		0.65		
201	1,3,5-triisopropylbenzene		0.68		
228	1,2,4-trimethylbenzene			1.46	
237	1,2,3,5-tetramethylbenzene	0.34	0.10	0.21	0.24
246	1,3-dimethyl-2,3-dihydro-1H-indene			0.32	

TABLE X.
NAMES AND CONTENT OF BICYCLIC AROMATIC HYDROCARBONS DETECTED WITH GC/MS

Peak	Names	Relative content (%)

number		SP_1	SP_2	SP_3	SP_4
53	1,2,3,4-tetrahydronaphthalene	0.14			
55	naphthalene	0.44			
66	6-methyl-1,2-dihydronaphthalene	0.51			
69	1-methylnaphthalene	0.41			
70	1,8-dimethl-1,2,3,4-tetrahydronaphthalene	0.33			
72	2-methylnaphthalene	0.79			
73	1,1,5-trimethyl-2,3-dihydro-1H-indene	0.32			
74	1,6,8-trimethyl-1,2,3,4-tetrahydronaphthalene	0.21			
79	1,6-dimethylnaphthalene	0.25			
80	1,3-dimethylnaphthalene	0.68			
81	2,7-dimethylnaphthalene	0.855			
82	2,3-dimethylnaphthalene	0.56	0.26		
87	2,3,6-trimethylnaphthalene	2.03			
88	1,6,7-trimethylnaphthalene	0.28			
89	7-isopropyl-1-methylnaphthalene	0.89			
91	4-isopropyl-1,6-dimethylnaphthalene	1.78			
95	1,4,5,8-tetramethylnaphthalene	0.43			
199	5,6,7,8-tetramethyl-1,2,3,4-tetrahydronaphthalene		0.56		

TABLE XI.
NAMES AND CONTENT OF TRICYCLIC AROMATIC HYDROCARBONS DETECTED WITH GC/MS

Peak number	Names	Relative content (%)			
		SP_1	SP_2	SP_3	SP_4
102	9-methylphenanthrene	0.29			
193	4H-cyclopenta[def]phenanthrene		0.69		
203	(4bS)-9-methyl-1,2,3,4,4a,4b,5,6-octahydrophenanthrene		0.45		

As shown in Table 12, a total of 9, 22, 21 and 16 phenolic compounds were detected in SP_1-SP_4, respectively, among which phenol and its homologues were the most abundant.. As Fig. 5 shows that phenolic compounds were detected in SP_2-SP_4 much higher than in SP_1. It can be inferred that methanol, ethanol, and isopropanol can break weak carbon-oxygen bonds due to nucleophilicity, resulting in the formation of phenolic compounds.

As shown in Table 13, esters are mainly alkyl esters distributed in SP_2-SP_4, and SP_3 is the most abundant. Cyclohexane cannot undergo ester exchange or esterification reactions with organic matter in coal, and the thermal treatment does not disrupt the interactions between ester compounds and the macromolecular structure of coal, hence no ester compounds were detected in SP_1. Methyl, ethyl, and propyl esters were detected in SP_2-SP_4.The result suggest that the ester compounds in SP_2-SP_4 are products of reactions involving solvents. Esters are not only obtained by the dissociation of small molecular esters existing in coal itself, but may also be obtained by the depolymer of reactions participated by solvents, they may be obtained by the esterification reaction of alcohols with carboxylic acids, or by the ester reaction of alcohols with ester bonds.

TABLE XII.
NAMES AND CONTENT OF PHENOLS DETECTED WITH GC/MS

Peak number	Names	Relative content (%)			
		SP_1	SP_2	SP_3	SP_4
26	phenol	0.27		0.11	0.73
33	o-cresol	0.49	0.50	0.19	1.63
37	p-cresol	0.43			1.10
47	2-ethylphenol	0.55		0.25	0.84
49	2,4-dimethylphenol	0.29		0.38	2.23
54	3,5-dimethylphenol	0.22	0.64	0.44	
61	2-ethyl-4-methylphenol	0.23			
62	2,4,6-trimethylphenol	0.09		1.27	3.99
64	4-isopropylphenol	0.17		0.20	
143	m-cresol		0.09	0.37	
147	2,3,5-trimethylbenzene-1,4-diol		3.09	0.57	1.88
148	2,6-dimethylphenol		2.47	0.15	
150	2-isopropyl-5-methylphenol		4.81	0.82	1.11
155	2,3,6-trimethylphenol		6.99		
160	3-ethyl-5-methylphenol		0.18		0.72
162	3,4,5-trimethylphenol		0.88		
165	4-isopropyl-3-methylphenol		1.81		
167	2-(tert-butyl)phenol		0.44		
170	4-methoxy-2,3,6-trimethylphenol		0.98		
172	2,3,4,6-tetramethylphenol		2.74		0.73
173	2-(tert-butyl)-6-methylphenol		1.04	0.32	
175	2-ethyl-5-propylphenol		0.37		
177	2-(tert-butyl)-5-methylphenol		0.56	0.31	
179	2,6-diisopropylphenol		0.52		
185	4-methyl-2-(pent-3-en-2-yl) phenol		0.96		
189	2-(tert-butyl)-4,6-dimethylphenol		0.63		
195	3,6-dimethyl-2-(2-methylbut-3-en-2-yl) phenol		0.57		
196	6,7-dimethylnaphthalen-1-ol		1.10		
200	2,5,8-trimethylnaphthalen-1-ol		0.54		
228	2,3,5-trimethylphenol			0.23	0.83
231	2,3,5,6-tetramethylphenol			0.80	1.34
243	3-ethylphenol			0.16	
244	Phenol, 3,4-dimethyl-			0.10	
252	2-ethyl-4,5-dimethylphenol			0.13	
254	4-(tert-butyl)-2-methylphenol			0.25	
255	5-isopropyl-2-methylphenol			0.32	
258	2-(tert-butyl)-4-methoxyphenol			0.34	
270	2,5-dimethylphenol				3.10
273	2-isopropylphenol				0.80
274	2,4,5-trimethylphenol				0.71
276	2,3-dimethylbenzene-1,4-diol				0.69

TABLE XIII.
NAMES AND CONTENT OF ESTERS DETECTED WITH GC/MS

Peak number	Names	Relative content (%)			
		SP_1	SP_2	SP_3	SP_4
115	methyl isobutyrate		1.51		
116	methyl butyrate		0.42		
120	methyl pentanoate		0.55		
128	methyl hexanoate		0.62		
138	methyl heptanoate		0.90		
146	methyl benzoate		0.38		

151	methyl octanoate	0.99	
153	methyl 2-methylbenzoate	0.29	
156	methyl 4-methylbenzoate	0.31	
158	methyl nonanoate	0.97	
169	methyl decanoate	0.44	
171	methyl 3,4-dimethylbenzoate	0.40	
183	methyl dodecanoate	0.41	
198	methyl tetradecanoate	1.60	
202	methyl palmitate	0.62	
206	methyl stearate	0.39	
210	ethyl propionate		0.97
214	ethyl butyrate		1.24
223	methyl 4-methylpent-4-enoate		0.58
226	ethyl hexanoate		5.35
229	ethyl hex-3-enoate		6.82
232	ethyl hex-2-enoate		6.71
238	ethyl heptanoate		0.20
248	ethyl octanoate		0.41
249	ethyl (E)-oct-2-enoate		0.44
250	ethyl 3-methylbenzoate		0.22
251	ethyl nonanoate		0.26
253	ethyl decanoate		0.19
263	isopropyl propionate		5.50
264	isopropyl butyrate		3.97
267	isopropyl pentanoate		1.01
269	isopropyl hexanoate		1.53
271	propyl heptanoate		0.78
272	isopropyl octanoate		0.65
275	isopropyl nonanoate		0.82

As shown in Table 14, alcohol compounds are distributed in SP_2-SP_4. Phenols are predominant in SP_2, while SP_3 is mainly composed of alkenols and phenols. One alkyl alcohol (2-methylpentan-2-ol) was detected in SP4. It is noteworthy that the relative content of alkenols in SP_2 reaches 37.85%, indicating that disrupting the interactions of alkenols with other functional groups requires the use of ethanol as a solvent for thermal dissolution to dissociate them.

As shown in Tables 15-16, typical NCOCs detected in SPs include pyridines, benzimidazoles, benzidines, and phenanthrolines. Among them, N1, N1, N4, N4-tetramethylbenzene-1,4-diamine has the highest content. A total of 16 SCOCs were detected, and dimethyl sulfide is the most abundant. As shown in the Table 17, a large number of ketone compounds were detected in SP_2-SP_3, which may be that a carboxylic acid reaction has occurred. This also confirms the reduction of the relative content of carboxylic acids in XPS.

TABLE XIV.
NAMES AND CONTENT OF ALCOHOLS DETECTED WITH GC/MS

Peak number	Names	Relative content (%)			
		SP₁	SP₂	SP₃	SP₄
118	2-methylpentan-3-ol		0.81		
126	1-methylcyclohexan-1-ol		0.12		
131	(R)-1-phenylethan-1-ol		0.28		
135	m-tolylmethanol		0.17		

136	(3,4-dimethylphenyl)methanol		0.14		
178	(4-(tert-butyl)phenyl)methanol		0.84	0.26	
208	2-methylprop-2-en-1-ol			33.60	
209	but-2-en-1-ol			4.35	
217	(E)-hex-3-en-1-ol			1.96	
218	2-methylpent-2-en-1-ol			1.10	
219	(E)-hex-2-en-1-ol			1.20	
220	hexan-1-ol			1.90	
224	5-ethylnonan-4-ol			0.25	
231	phenylmethanol			0.66	
240	p-tolylmethanol			0.36	
241	o-tolylmethanol			0.46	
261	2-methylpentan-2-ol				0.91

TABLE XV.
NAMES AND CONTENT OF NCOCS DETECTED WITH GC/MS

Peak number	Names	Relative content (%)			
		SP₁	SP₂	SP₃	SP₄
58	5,6-dimethyl-1H-benzo[d]imidazole	0.56	0.21		
127	2-ethylpyridine		0.12		
139	4-isopropylpyridine		0.16		
152	N, N, 3,5-tetramethylaniline		0.21		
182	2,3,4,5,6-pentamethylpyridine		0.39		
184	N1, N1, N4, N4-tetramethylbenzene-1,4-diamine		6.00		
207	2-isopropyl-3-phenylquinoxaline		0.70		
234	4-propylpyridine			0.18	

TABLE XVI.
NAMES AND CONTENT OF SCOCS DETECTED WITH GC/MS

Peak number	Names	Relative content (%)			
		SP₁	SP₂	SP₃	SP₄
121	(methylsulfinyl)methane		1.50		
133	1-(sec-butyl)-2-ethyldisulfane		0.08		
157	2-isopropylbenzenethiol		0.25		
180	methyl(p-tolylethynyl)sulfane		0.54		
181	4-(tert-butyl)benzenethiol		0.47		
188	2,5,7-trimethylbenzo[b]thiophene		0.60		
192	2-ethyl-7-methylbenzo[b]thiophene		0.54		
194	2-ethyl-5,7-dimethylbenzo[b]thiophene		1.22		
222	1,2-diethyldisulfane			0.42	
225	3-methylbutanethial			0.45	
230	dimethylsulfane			2.56	

TABLE XVII.
NAMES AND CONTENT OF OCOCS DETECTED WITH GC/MS

Peak number	Names	Relative content (%)			
		SP₁	SP₂	SP₃	SP₄
44	2-methylbenzofuran	0.69			
137	1-methoxy-4-methylbenzene		0.17		
161	1-isopropyl-2-methoxy-4-methylbenzene		0.17		
166	4-isopropylbenzoic acid		0.73		
174	5-propylbenzo[d][1,3]dioxole		0.62		
176	2-ethyl-1,4-dimethoxybenzene		0.91		
212	3-methyl-2,3-dihydrofuran			0.73	
216	2-ethylbut-2-enal			1.15	

221	(2E,4E)-hexa-2,4-dienal	1.00
233	octa-2,4,6-trienal	0.29
235	2-methylbenzaldehyde	0.51
236	4-methylbenzaldehyde	0.31
242	1-(ethoxymethyl)-2-methylbenzene	0.16
245	1-ethyl-4-methoxybenzene	0.25
268	4-methylpent-2-enoic acid	0.15

TABLE XVIII.
NAMES AND CONTENT OF OCOCS DETECTED WITH GC/MS

Peak number	Names	Relative content (%)			
		SP_1	SP_2	SP_3	SP_4
117	2-methylpentan-3-one		2.45		
119	2,4-dimethylpentan-3-one		0.71		
124	2,5-dimethylcyclopentan-1-one		1.44		
129	2,3-dimethylcyclopent-2-en-1-one		2.36		
132	2,4-dimethylheptan-3-one		0.09		
134	2,6-dimethylcyclohexan-1-one		0.16		
142	3,4,4-trimethylcyclopent-2-en-1-one		2.13		
149	2,3,4,5-tetramethylcyclopent-2-en-1-one		1.93		
159	6,6-dimethyl-5-methylenehept-3-en-2-one		0.21		
163	2-isopropyl-5-methylcyclohexan-1-one		0.66		
187	1-(3,5-dimethoxyphenyl)ethan-1-one		0.77		
191	1-(5-hydroxy-2,3,4-trimethylphenyl)ethan-1-one		1.25		
256	1-(2,4-dihydroxy-3-methylphenyl)ethan-1-one			0.29	
257	1-(2-hydroxy-6-methoxyphenyl)ethan-1-one			0.44	
262	4-methylpentan-2-one				0.82
265	hex-3-en-2-one				3.35

CONCLUSION

According to TGA analysis, the thermal decomposition behavior of NL in the range was 100-900 °C, and it was found that total weight loss of the coal sample was 45%, and the weight loss rate was the largest in the range of 420-700℃ about 40%. Through the fitting of the DTG curve of the coal sample, it was found that NL underwent a strong bond breaking process between 400-500 °C, mainly the breakage of covalent bonds such as Calk-C, Calk-H, Cak-O and Car-N. According to ultimate analysis, after sequential thermal dissolution, while the O content decreases significantly, indicating that sequential thermal dissolution has a good effect on the dissolution of oxygen compounds or oxygen bridges in coal. According to XPS and FTIR analysis, COOH content decreases significantly. By GC/MS, compounds detected in SP_1 are mainly alkanes, alkenes, and aromatics, while phenols predominant in SP_2, alcohols and esters are dominant in SP_3, and alkanes are mainly found in SP_4. It is noteworthy that NCOCs relatively high in SP_2, and SCOCs were detected only in SP_2 and SP_3. According to the solubility rules of aromatic hydrocarbons, it is speculated that there two possible sources of aromatic hydrocarbons: one is from the aromatic hydrocarbons existing in the structure of NL itself; on the other hand, since the aromatic hydrocarbons in the hot solvents are mostly methyl-substituted aromatic hydrocarbons, they be due to the breakage of the C_α-C_β bond of the straight-chain alkylbenzene at high temperature. The steric hindrance and nucleophilicity of alcohol solvents are different, and the dissociation energies of different types of oxygen bridge bonds are also different, which will affect the type of oxygen bridge bonds attacked in the sequential thermal dissolution process, so that different hot solution products will be obtained.

References

[1] Shao.Junjie, The current situation of brown coal upgrading technology and the preliminary exploration of the development trend of brown coal upgrading technology in China, Shenhua Technology, 2009, 7(2): 17-22.
[2] Schobert. H H, Song. C, Chemicals and materials from coal in the 21st century, Fuel, 2002, 81(1): 15-32.
[3] Rao. Z, Zhao. Y, Huang. C, Duan. C, Recent developments in drying and dewatering for low rank coals, Progress in Energy and Combustion Science, 2015, 46: 1-11.
[4] Li. Y, Huang. S, Wu. Y, Gao. J, The roles of the low molecular weight compounds in the low-temperature pyrolysis of low-rank coal, Journal of the Energy Institute, 2019, 92(2): 203-209.
[5] Xiong. Y, Jin. L, Li. Y, Yang. Z, Structural Features and Pyrolysis Behaviors of Extracts from Microwave-Assisted Extraction of a Low-Rank Coal with Different Solvents, Energy & Fuels, 2019, 33(1): 106-114.
[6] Lou. Z, Cheng. Z, Sun. K, Wang. Z, Jin. Y, Ma. C, Bai. X, Analysis of pyrolysis and combustion characteristics of several coals with different coal properties, Journal of Physics: Conference Series., 2683, 2683(1).
[7] Zhao. Y P, Xiao. J, Ding. M, G. E, Eddings, Wei. X Y, Fan. X, Zong. Z M, Sequential Extraction and Thermal Dissolution of Baiyinhua Lignite in Isometric CS2/Acetone and Toluene/Methanol Binary Solvents, Energy & Fuels, 2016, 30(1): 47-53.
[8] Ding. S H, Gu. M Y, Jia. Y D, Chang. T, Wang. G, Tang. C, Research Progress in Pyrolysis of Low-Rank Coals under Different Conditions, Advanced Materials Research, 2014, 953-954: 1131-1134.
[9] Lv. J H, Wei. X Y, Zhang. Y Y, Zong. Z M, Zhang. Y L, Ma. M J, Bai. H C, Benzenecarboxylic acid production by oxidation of Shenmu char powders with aqueous sodium hypochlorite, Fuel, 2020, 278: 118194.
[10] Lv. J H, Wei. X Y, Wang. Y H, Wang. T , Liu. J, Zhang. D D, Zong. Z M, uctural features of Zhundong subbituminous coal through ruthenium ion-catalyzed oxidation, RSC Advances, 2016, 6(15): 11952-11958.
[11] Kang. H, Chen. F, Rong. T, Wang. J X, Guo. H, Yu. H F, Zuo. H B, Investigation of solvothermal extraction of direct coal liquefaction residue by macromolecular models, Separation and Purification Technology, 2024, 340: 126781.
[12] Okuma. O, Liquefaction process with bottom recycling for complete conversion of brown coal, Fuel, 2000, 79(3): 355-364.
[13] Zhang. Y Y, Wei. X Y, Lv. J H, Jiang. H, Liu. F J, Liu. G H, Identification of oxygen-containing aromatics in soluble portions from thermal dissolution and alkanolyses of Baiyinhua lignite, Fuel Processing Technology, 2019, 186: 149-155.
[14] Yoshida. T, Li. C, Takanohashi. T, Matsumura. A, Sato. S, Saito. I, Effect of extraction condition on "HyperCoal" production (2)—effect of polar solvents under hot filtration, Fuel Processing Technology, 2004, 86(1): 61-72.
[15] Li .Z K, Wei. X Y, Yan. H L, Yu. X Y, Zong. Z M, Characterization of soluble portions from thermal dissolution of Zhaotong lignite in cyclohexane and methanol[J]. Fuel Processing Technology, 2016, 151: 131-138.
[16] Li. Z K, Zong. Z M, Yan. H L, Wang. Y G, Ni. H X, Wei. X Y, Li. Y H, Characterization of acidic species in ethanol-soluble portion from Zhaotong lignite ethanolysis by negative-ion electrospray ionization Fourier transform ion cyclotron resonance mass spectrometry, Fuel Processing Technology, 2014, 128: 297-302.
[17] Zhang. Y Y, Zong. Z M, Sun. Y B, Investigation on the structural feature of Shengli lignite, International Journal of Mining Science and Technology, 2018, 28(2): 335-342.
[18] Shi. L, Liu. Q, Guo. X, Wu. W Z, Liu. Z Y. Pyrolysis behavior and bonding information of coal — A TGA study, Fuel Processing Technology, 2013, 108: 125-132.
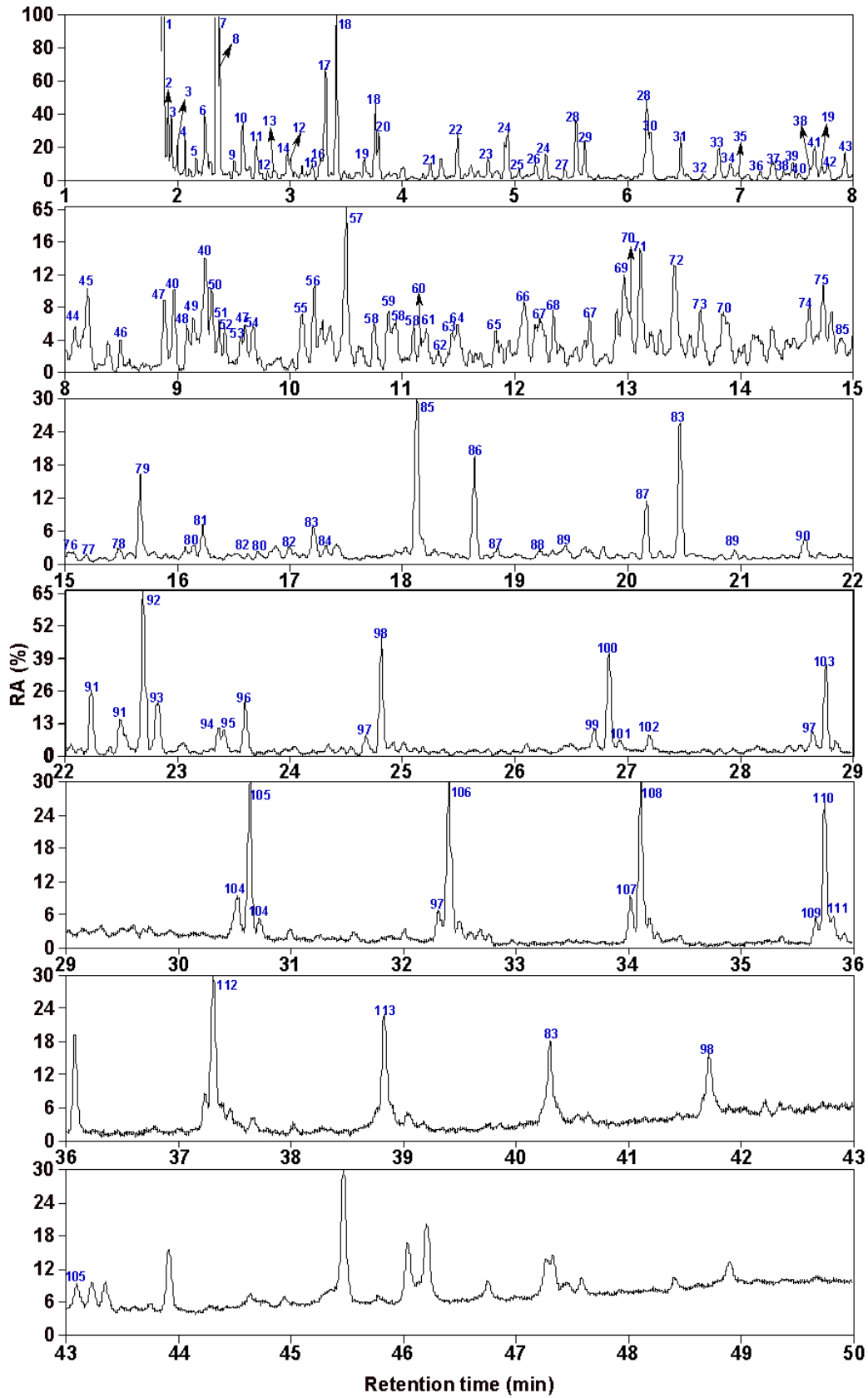
Fig.6. Total ion chromatogram of SP_1 from thermal dissolution of NL
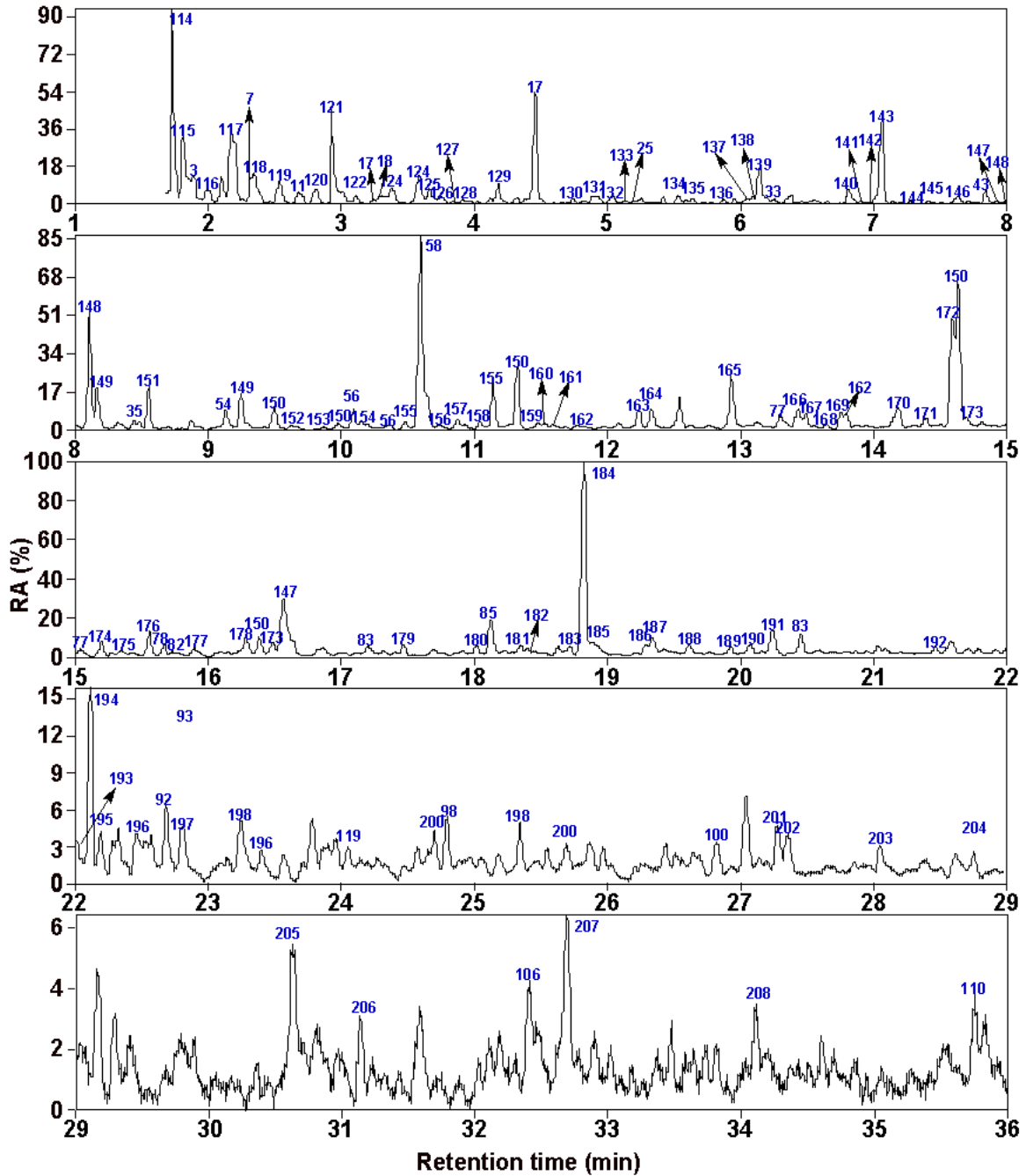
Fig.7. Total ion chromatogram of SP_2 from thermal dissolution of NL
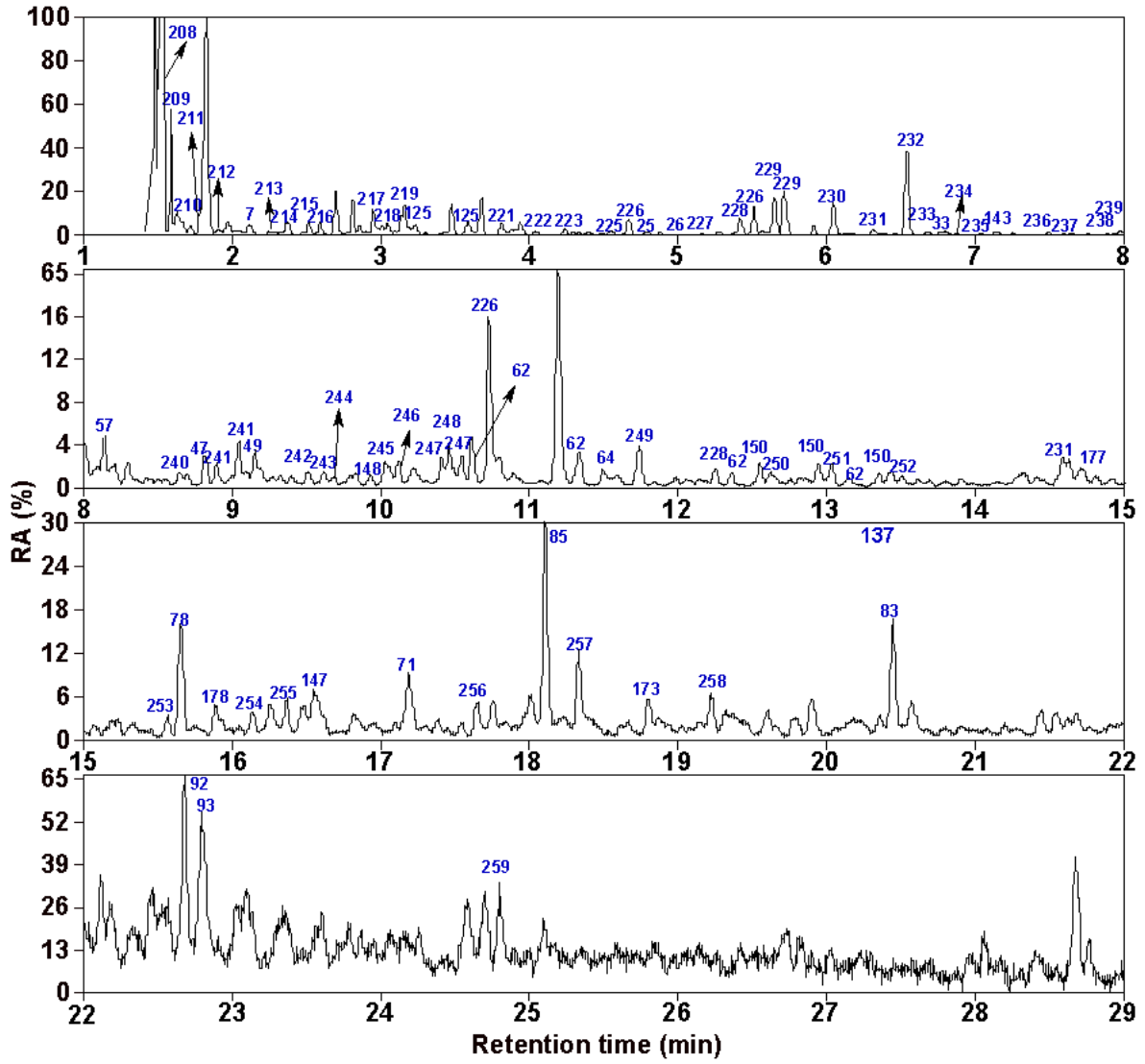
Fig.8. Total ion chromatogram of SP_3 from thermal dissolution of NL
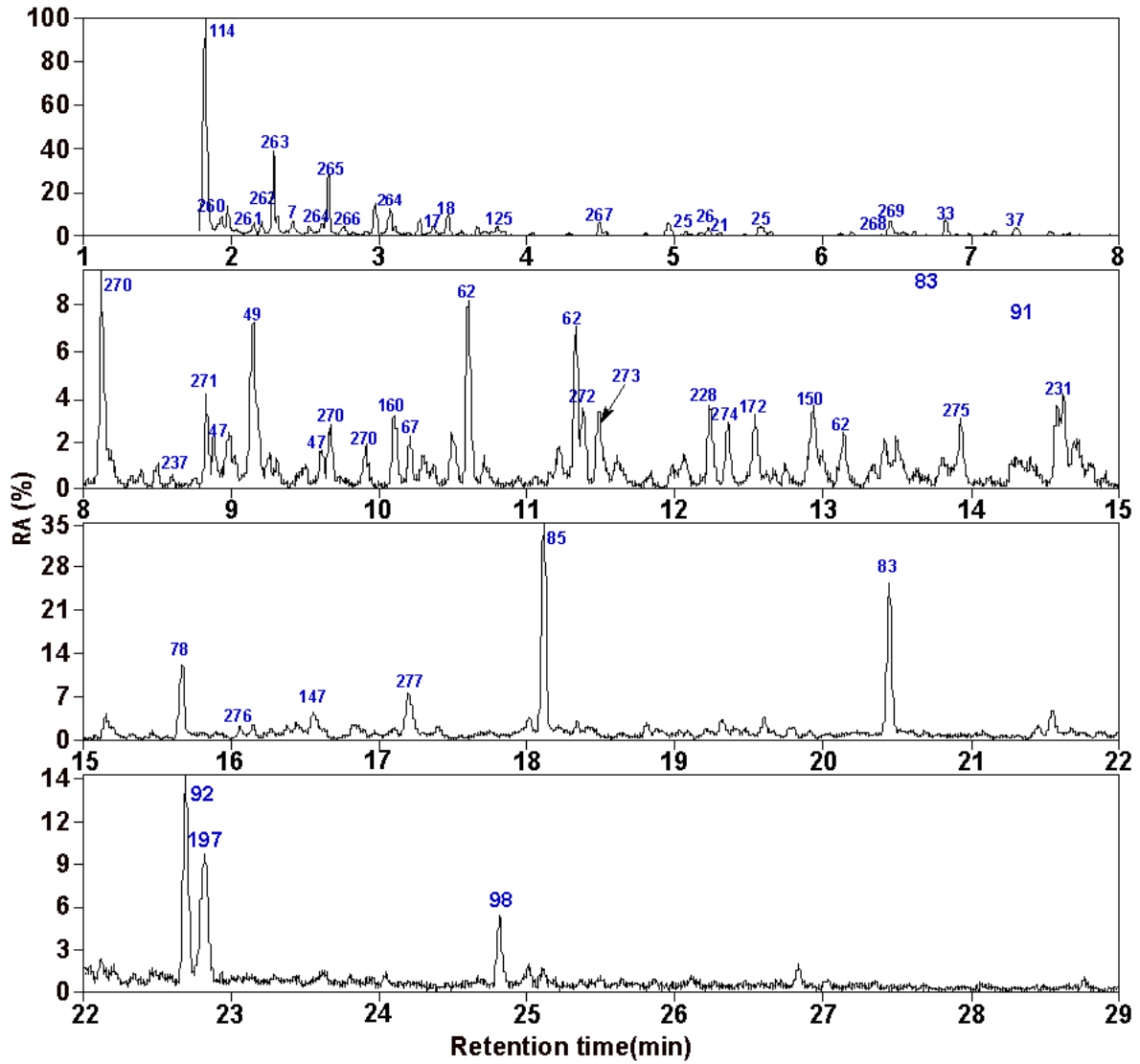
Fig.9. Total ion chromatogram of SP_4 from thermal dissolution of NL